

UNIVERSITY OF CALIFORNIA
SANTA CRUZ

FASTPAS - FAST PREDICTIVE AERIAL SCANNING

A thesis submitted in partial satisfaction of the
requirements for the degree of

MASTER OF SCIENCE

in

COMPUTER ENGINEERING

with an emphasis in

ROBOTICS AND CONTROL

by

Sargis S Yonan

June 2018

The Dissertation of Sargis S Yonan
is approved:

Professor Gabriel Hugh Elkaim, Chair

Professor Numero Dos

Professor Numero Tres

Dean Tyrus Miller
Vice Provost and Dean of Graduate Studies

Copyright © by

Sargis S Yonan

2018

Table of Contents

List of Figures	vi
List of Tables	vii
Abstract	viii
Dedication	x
Acknowledgments	xi
 I Background	 1
1 Geostatistical Interpolation	2
1.1 Tobler's First Law of Geography	2
1.1.1 Measuring and Estimating Points of Interest in a Field	3
1.1.2 Stochastic Field Notation	4
1.1.3 Autocorrelation in a Field	4
1.2 Inverse Distance Weighting	5
1.3 Variography	7
1.3.1 The Variogram	7
1.3.2 The Semi-Variogram	8
1.3.3 Converting a Semi-Variogram to a Variogram	10
1.3.4 Range, Sill, and Nugget	10
1.3.5 Statistical Models	10
1.3.6 Fitting A Semi-Variogram	10
1.4 Covariance-Variance Matrix	12
1.5 The Kriging Method	12
1.5.1 A Best Linear Unbiased Predictor	12
1.5.2 Exploiting Geospatial Autocorrelation	12
1.6 Forms of the Kriging Method	12
1.7 The Kriging Formula	12
1.8 The Kriging Prediction	12

2	Optimization of Interpolation Methods	14
2.1	Natural Neighbor Selection	14
2.1.1	Finding Natural Neighbors	14
3	Required Graph Theory	15
3.1	Graph Construction	15
3.1.1	Vertices and Edges	15
3.1.2	Path Problems	15
II	Efficient Interpolation	16
4	Introduction	17
4.1	Kriging Prediction	17
4.1.1	Variography in Kriging Weight Selection	18
4.1.2	Semi-Variogram	19
4.1.3	Variogram	19
4.1.4	Choosing Kriging Weights	19
4.1.5	Measuring Prediction Confidence	19
4.1.6	Drawbacks To The Kriging Method	19
4.2	Natural Neighbor Selection	20
4.2.1	Voronoi Tessellations	20
III	Autonomous Path Finding	21
4.2.2	Constructing a Confidence Graph	22
4.2.3	Confidence Optimized Path Finding	22
5	Previous Work	23
IV	Can it fly?	24
6	Introduction	25
6.1	Custom Simulation	25
6.1.1	Flying Engine	25
6.2	FastPAS	25
6.2.1	The Algorithm	25
6.2.2	Simulating It	25
6.3	Other Uses	25
7	Results	26
8	Conclusion	27
	Bibliography	28

List of Figures

1.1	A Gaussian distributed randomly generated spatially autocorrelated field created using <i>MATLAB</i>	5
1.2	A randomly generated field where 250 observations were made (left), and an Inverted Distance Weighted Prediction (right) of that field	6
1.3	An empirical variogram generated using Equation 1.5 on the field and random samples previously generated in Figure 1.2a. δ was chosen such that for n observations, a total number of $\left\lfloor \frac{n}{2} \right\rfloor$ points were plotted	9
1.4	A comparison of the Gaussian, Spherical, and Exponential statistical models fit to the Empirical Variogram in Figure 1.3	11
1.5	A randomly generated field where 250 observations were made (left), and a Kriging Prediction (right) of that field from the marked observations. . . .	12
1.6	A randomly generated field where 250 observations were made (left), and a Kriging Prediction (right) of that field from the marked observations. . . .	13

List of Tables

Abstract

FASTPas - Fast Predictive Aerial Scanning

by

Sargis S Yonan

Unmanned Aerial Vehicles (UAVs) have become more prevalent in fields of work and study that benefit from having a birds eye view on a given situation. Firefighter teams have been using UAVs to find the origin of fires, and where fires are spreading to. Scientific researchers have been using aerial thermal imaging to determine rates of change in ice growth and melting, and thermal exchange between the ocean and atmosphere.

The use of autonomous UAVs could benefit rescue teams, firefighters, scientific researchers, and private sector industries in the interest of time and data discovery. Using a single or multiple UAVs in a flying network, an area with fields of interest can be scanned efficiently completely autonomously. By simply drawing on a map the general area wished to be scanned by the autonomous fleet, a deployed pod of these UAVs can stream back, to a ground station, live aerial information. This mapping time can be greatly reduced with the use of statistical interpolation techniques that help the pod or single UAV avoid having to scan an entire region, but rather, have the UAVs scan the areas with the lowest level of confidence in prediction.

The Kriging Method, a popular interpolation tool offers a prediction and a variance of prediction, but is computationally expensive because of constant fitting procedures. We can exploit the Kriging variances generated by our prediction to motivate the UAVs to

autonomously steer in the areas of least confidence until a minimum confidence in prediction is achieved for an entire unknown field. By designing a computational efficient algorithm based on a Universal Kriging Method, the system is feasible and could benefit a large group of potential users.

To all who think flying robots are cool

Acknowledgments

I want to thank Sharon Rabinovich, who reminded me: "Although a cow is tied up, it still wants eat grass."

Part I

Background

Chapter 1

Geostatistical Interpolation

Stochastic fields are areas where...we can predict if we take advantage of...

1.1 Tobler's First Law of Geography

We will exploit several concepts developed in the field of Geostatistics and Geography to assist our path finding and aerial prediction system. Tobler's First Law of Geography [5] states, "Everything is related to everything else, but near things are more related than distant things." Regarding geospatial data, we can say at the very least, there is a positive correlation between entities that are closely related in distance [3]. This implies the existence of geospatial autocorrelation, or a positive correlation between elements in a series, spatially, in this case for our observed geographies. We can exploit this fundamental law of Geography for geostatistical interpolation methods like inverse distance weighting. Furthermore, if we view our observed fields as an unknown stochastic process, with a generally known underlying statistical model, there exists an overall trend with correlated variation

between observed points. We can use these additional caveats to create a Best Linear Unbiased Predictor (BLUP) which can robustly predict intermediate spatial points between observations alongside an additional measure of confidence via a weighted least-squares calculation. We will exploit these geostatistical processes to construct graphs of confidence for flight planning, and to predict unknown fields, aerially using UAVs, to some degree of confidence.

1.1.1 Measuring and Estimating Points of Interest in a Field

The basis of our predictions will be observations we make using reliable sensors. For the methods we will explore and develop, we must estimate the coordinates likely using The Global Positioning System for each point of interest we measure. In order to use the techniques we will explore we must assume that we can get a Euclidean distance between any two measured points. If a GPS sensor is used to estimate position, we will likely use a Haversine Transformation to convert Earth longitude and latitude estimated by our sensor to points on a Cartesian plane where we will represent our measurements. For each coordinate measured, we will also need to measure some value of interest. If tracking and predicting the current location of a wildfire, for example, we will likely use an infrared sensor to measure the thermal output of the field in which we would like to predict. We will assume that the points of interest will be measured with little to no error, and our coordinate system is on a Cartesian plane with Euclidean distances separating points on a generic unit-distance scale.

1.1.2 Stochastic Field Notation

For the sake of convention throughout this work, we will denote $\begin{bmatrix} x_1 & x_2 \end{bmatrix}^T$ to be a column vector of position measurements on the domain (where x_1 is measured) and co-domain (where x_2 is measured) of the Cartesian plane representing a topological field respectively. The i^{th} row of the matrix $X = \begin{bmatrix} \mathbf{x}_1 & \mathbf{x}_2 \end{bmatrix}^T$, as a point-pair denoted as $\mathbf{X}_i = \begin{bmatrix} \mathbf{X}_{1_i} & \mathbf{X}_{2_i} \end{bmatrix}^T$, will represent the location of the i^{th} observed location on the Cartesian plane.

We will denote the vector, \mathbf{u} , to be a vector of our measured values at our i^{th} observation, $u_i \in \mathbb{R}$, a non-location measurement of interest (e.g. an infrared sensor measurement). For an enclosed neighborhood of points, D , in a stochastic field, Z , we will define $Z(\mathbf{X}_i) : \mathbf{X}_i \rightarrow \mathbb{R}$, $\mathbf{X}_i \in D \subset \mathbb{R}^2$. The i^{th} element of \mathbf{u} , u_i , a random variable in a stochastic process, or field, Z , will correspond to a scalar observation located at $[x_{1_i} \ x_{2_i}]^T$. Giving us, $Z(\mathbf{X}_i) = u_i$. We will denote a predicted value on a field to be $\hat{Z}(\mathbf{X}_i) = \hat{u}_i$.

1.1.3 Autocorrelation in a Field

Positively correlated geospatial autocorrelation in a field implies the existence of a cluster of similar observed values near one another. The opposite is true when the overall geospatial autocorrelation of a field is negative. We can assume, from Tobler's First Law of Geography, that the fields we will measure will contain positive autocorrelation. This degree of geospatial autocorrelation can be measured, and will be discussed in the subsection on variography.

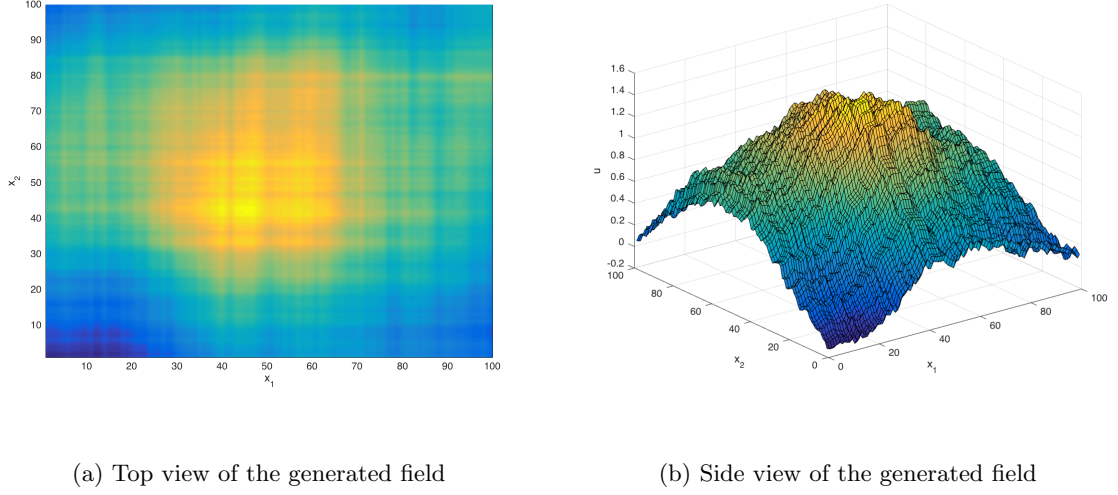


Figure 1.1: A Gaussian distributed randomly generated spatially autocorrelated field created using *MATLAB*

1.2 Inverse Distance Weighting

A simple Inverse Distance Weighting (IDW), using Shepard's Method [4], gives us a prediction of an unobserved point, \hat{u}_j , at location \mathbf{X}_j , defining $\hat{Z}(\mathbf{X}_j)$ to be:

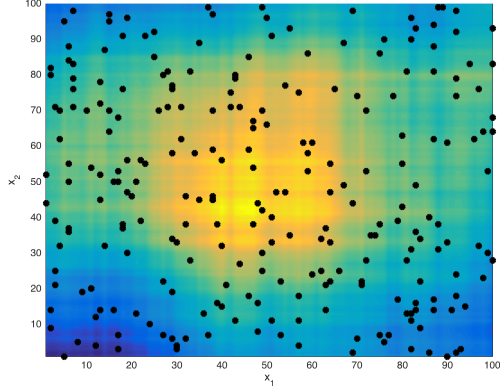
$$\hat{Z}(\mathbf{X}_j) = \begin{cases} \frac{\sum_{i=1}^N w(\mathbf{X}_j, \mathbf{X}_i) u_i}{\sum_{i=1}^N w(\mathbf{X}_j, \mathbf{X}_i)} & \text{if } \forall i \mid d(\mathbf{X}_j, \mathbf{X}_i) \neq 0 \\ u_j & \text{if } \exists i \mid d(\mathbf{X}_j, \mathbf{X}_i) = 0 \end{cases} \quad (1.1)$$

$$w(\mathbf{X}_j, \mathbf{X}_i) = \frac{1}{d(\mathbf{X}_j, \mathbf{X}_i)^p} = \|\mathbf{X}_j - \mathbf{X}_i\|_2^{-p} \quad (1.2)$$

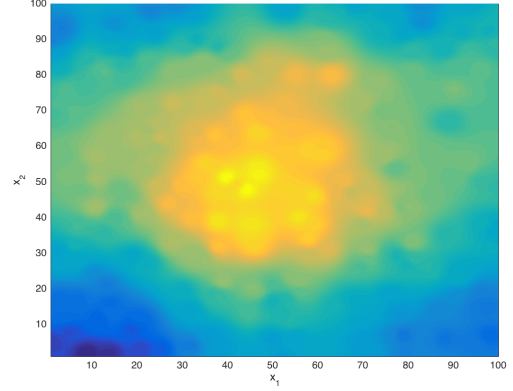
where $p \in \mathbb{R}^+$ is the IDW "power parameter". The power parameter, p , controls the emphasis on near and far observations on a prediction. As p increases, the predicted values more closely resemble the closest made observation to the prediction location. Inversely, as p gets smaller within $(0, 1]$, more emphasis is drawn from observations made further away.

In order to apply the Inverse Distance Weighting prediction method to the previously

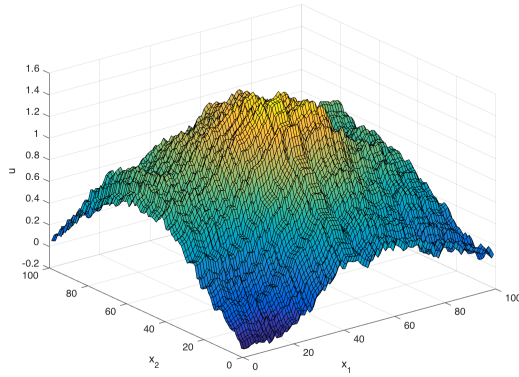
generated map, we will first generate a random set of sample points.



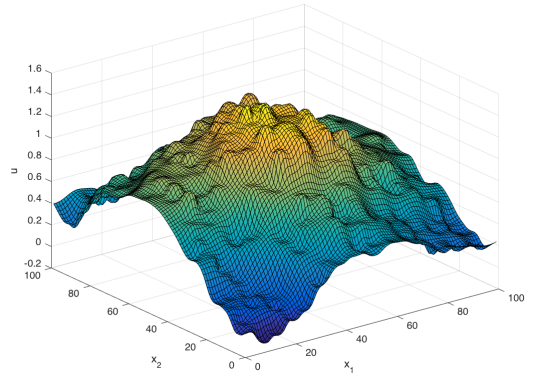
(a) Sampled locations (250 points marked in black) of the previously generated geospatially autocorrelated field in Figure 1.1a



(b) An Inverse Distance Weighting generated predicted field ($p = 3$). Generated from 250 random observations made in Figure 1.2a



(c) A side view of the previously generated geospatially autocorrelated field in Figure 1.1b



(d) A side view of the IDW generated in Figure 1.2b

Figure 1.2: A randomly generated field where 250 observations were made (left), and an Inverted Distance Weighted Prediction (right) of that field

This method can give us a prediction for all possible \mathbf{X}_j points in a field where a set of observations at labeled positions were made, as done in Figure 1.2. Unfortunately, the method is limited in that it does not take advantage of the underlying stochastic model of the field, Z , being observed. We will further expand on this method to exploit the fact that Z is a stochastic process with underlying geospatially autocorrelated random variables.

1.3 Variography

Variography is a set of procedures for examining and interpreting spatial dependence and geospatial autocorrelation in observed data. We would like to unravel the autocorrelation, or spatial dependence, of observed data to factor into a classical Inverse Distance Weighting, yielding a Best Linear Unbiased Predictor. The heart of variography is the Variogram Function, a function which quantifies dependence for observed data separated by some vector distance and angle, i.e. the covariance between two given points in a stochastic field. We will develop the basis for the Variogram function and fit our sampled observations to a continuous Variogram model.

1.3.1 The Variogram

A Variogram is intended to be a continuous function which yields a covariance between two points $Z(\mathbf{X}_i)$, $Z(\mathbf{X}_j)$, which were not necessarily observed, but known to be a vector $\mathbf{h} \in \mathbb{R}^2$ apart. Using the assumption made in Equation 2.4.1 of Matherson, 1963 [2]:

$$Z(\mathbf{X}_i) = \mu(\mathbf{X}_i) + \delta(\mathbf{X}_i) \tag{1.3}$$

Where $\delta(\cdot)$ is a zero-mean intrinsically stationary stochastic process, which our observations in a field Z are therefore expected to be. If we assume a mean $\mu(\cdot)$ is only constant in a reasonably small neighborhood, a modified version of the variogram definition in equation 2.3.4 of Matherson, 1963 [2] is defined to be:

$$2\gamma(\mathbf{X}_i, \mathbf{X}_j) = \text{var}(Z(\mathbf{X}_i) - Z(\mathbf{X}_j)) = E[((Z(\mathbf{X}_i) - \bar{Z}) - (Z(\mathbf{X}_j) - \bar{Z}))^2] \quad (1.4)$$

Where \bar{Z} is the mean of the observations made in a stochastic field, Z , for a reasonably small neighborhood of points.

It is infeasible and impossible to estimate an observation value at each possible point to compute a continuous variogram. We must therefore define a discrete model which will be fit into a continuous variogram model.

1.3.2 The Semi-Variogram

A Semi-Variogram, or Empirical Variogram, is a discrete function representing the covariance of the observation value difference between two sampled locations that are some vector \mathbf{h} apart. By modifying equation 2.4.2, Matheron, 1963 [2] to include an additional boundary to classify a "bin", for two observations $\mathbf{X}_i, \mathbf{X}_j$ in a stochastic field, Z , the empirical semivariogram is defined to be:

$$2\hat{\gamma}(\mathbf{h} + \boldsymbol{\delta}) := \frac{1}{|N(\mathbf{h} + \boldsymbol{\delta})|} \sum_{(i,j) \in N(\mathbf{h} + \boldsymbol{\delta})} |Z(\mathbf{X}_i) - Z(\mathbf{X}_j)|^2 \quad (1.5)$$

Where $N(\mathbf{h} + \boldsymbol{\delta})$ is the number of pairs of observed data locations that are a vector distance and angle $\mathbf{h} + \boldsymbol{\delta}$ apart, and $\boldsymbol{\delta} = \begin{bmatrix} \pm\delta & \pm\delta \end{bmatrix}^T$ is a bound of ranges acceptable to be

”binned” alongside \mathbf{h} .

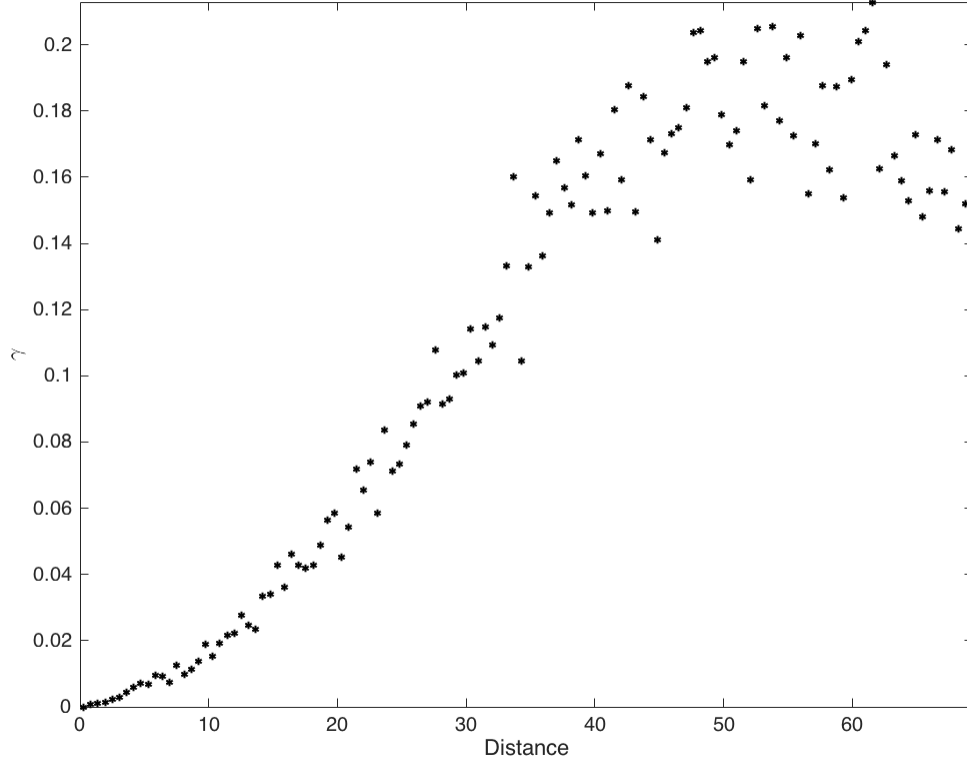


Figure 1.3: An empirical variogram generated using Equation 1.5 on the field and random samples previously generated in Figure 1.2a. δ was chosen such that for n observations, a total number of $\left\lfloor \frac{n}{2} \right\rfloor$ points were plotted

The plot of the empirical variogram in figure 1.3 conveys to us the geospatial autocorrelation of the sampled field that was previously generated in figure 1.2a. We can see that as the distance, $\|\mathbf{h}\|_2$, between two given points increases, the covariance also increases. At some point in the graph the covariance levels out to a steady value (the sill) at some distance in the domain (the range). This informs us of locations of where the loss of reliable geospatial autocorrelation between two points that are a vector distance \mathbf{h} apart lies. This

will later act as a method of prediction confidence in our Best Linear Unbiased Predictor.

1.3.3 Converting a Semi-Variogram to a Variogram

The objective of fitting a statistical model to an empirical variogram is to approximate the continuous covariance for any two points on Z that are at some known \mathbf{h} apart, i.e. to obtain a decent approximation of equation 1.4.

1.3.4 Range, Sill, and Nugget

1.3.5 Statistical Models

objective functions

The Gaussian Model

The Exponential Model

The Spherical Model

Other Models

1.3.6 Fitting A Semi-Variogram

fminsearchbound

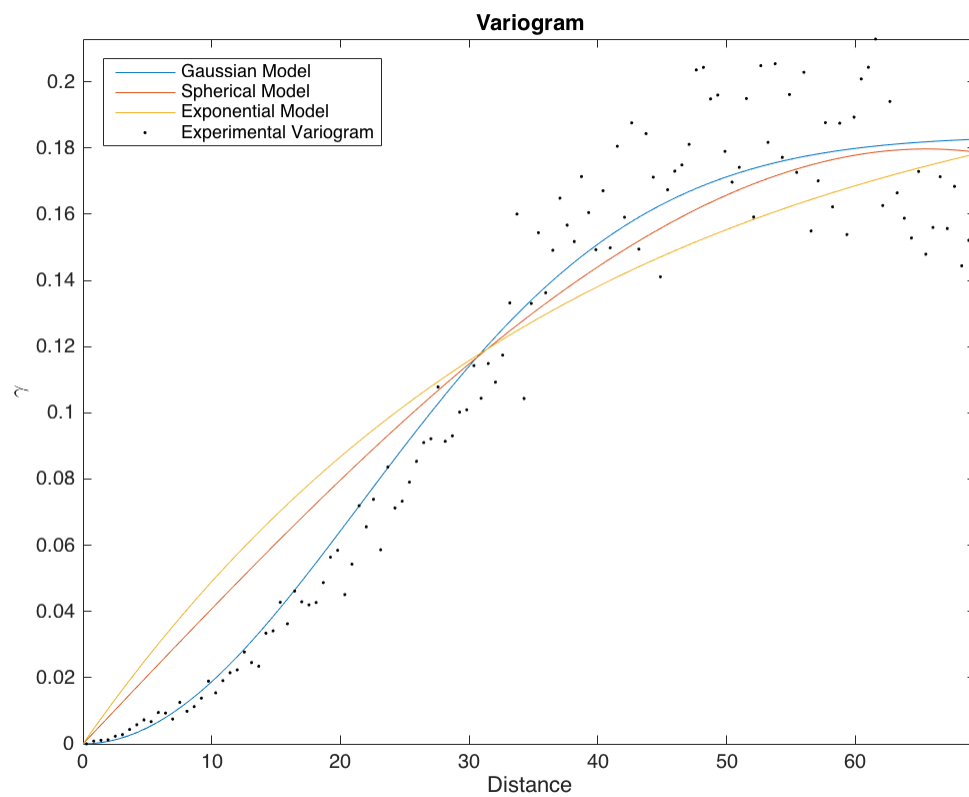


Figure 1.4: A comparison of the Gaussian, Spherical, and Exponential statistical models fit to the Empirical Variogram in Figure 1.3

1.4 Covariance-Variance Matrix

1.5 The Kriging Method

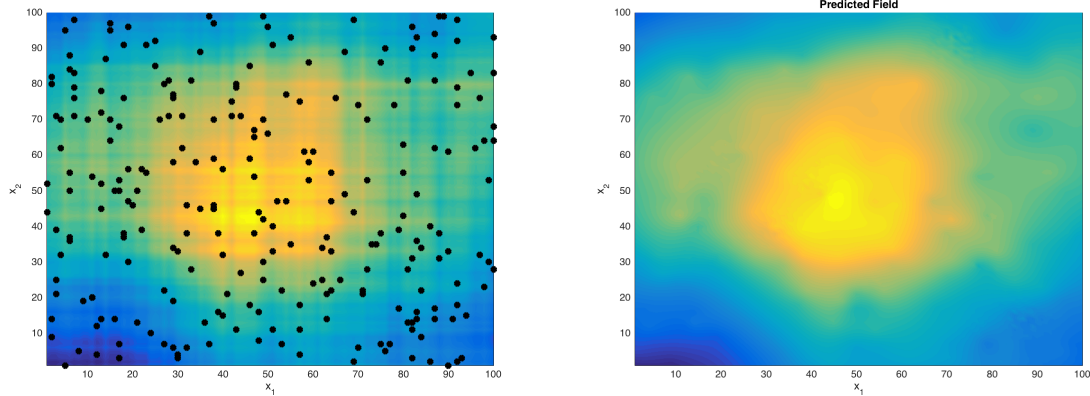
1.5.1 A Best Linear Unbiased Predictor

1.5.2 Exploiting Geospatial Autocorrelation

1.6 Forms of the Kriging Method

1.7 The Kriging Formula

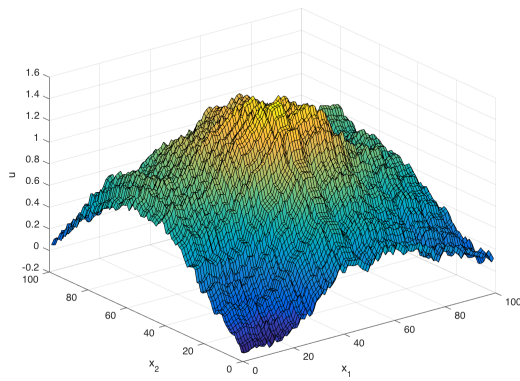
1.8 The Kriging Prediction



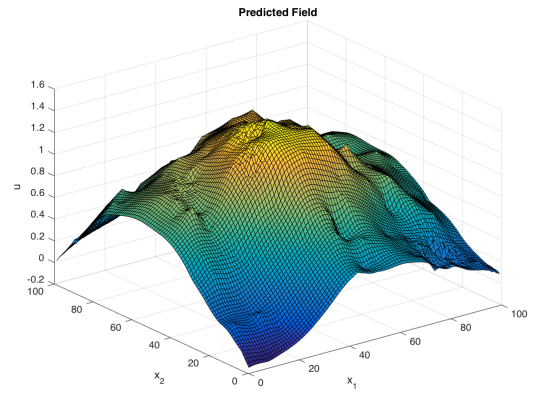
(a) Sampled locations (250 points marked in black) of the previously generated geospatially autocorrelated field

(b) A Kriging Prediction of the originally generated random field

Figure 1.5: A randomly generated field where 250 observations were made (left), and a Kriging Prediction (right) of that field from the marked observations.



(a) A side view of the previously generated geospatially autocorrelated field



(b) A Kriging Prediction of the originally generated random field

Figure 1.6: A randomly generated field where 250 observations were made (left), and a Kriging Prediction (right) of that field from the marked observations.

Chapter 2

Optimization of Interpolation

Methods

2.1 Natural Neighbor Selection

2.1.1 Finding Natural Neighbors

Chapter 3

Required Graph Theory

3.1 Graph Construction

3.1.1 Vertices and Edges

3.1.2 Path Problems

Optimizing a Route

Part II

Efficient Interpolation

Chapter 4

Introduction

There currently exists no consumer-level UAV system that can autonomously scan a perimeter of area to quickly map an unknown field. Due to the benefits of the solution to the problem, in terms of scientific research and benefit to fire fighting, I believe that designing a modified mathematical statistical interpolation method could make this system possible. Using a modified Kriging Method and a custom autonomous pod-UAV simulation, I would like to demonstrate that the system is possible, and could also benefit a variety of civil servants and scientists. We will, in this chapter, develop the tools and understanding of a method for interpolating data autonomously from just a few measured positions.

4.1 Kriging Prediction

It can be impossible to scan every square unit of area in a field, even with UAVs. Depending on the size of the map, it can often be most beneficial, in the interest of time flying above an area, to get a good enough prediction of the status of a field based off of a limited

number of samples.

The Universal Kriging Method, also known as the WienerKolmogorov prediction, is a geo-statistical Gaussian process interpolation method historically used in fields varying from natural resource location prediction for mining to real estate value appraisals.

Using the Kriging method, the unknown prediction of interest at point s_0 is achieved via:

$$\tilde{Z}(s_0) = \sum_{i=1}^n \lambda_i Z(s_i) \quad (4.1)$$

where λ_i is the Kriging weight associated with the sampled point at $Z(s_i)$.

The Kriging method fits values to the λ_i weights using information interpreted from the field as data comes into the system.

4.1.1 Variography in Kriging Weight Selection

The factors that play into the calculations of these weights come from the variances of disjoint points sampled in the fields as well as factors inversely proportional to the square distances of the point in question and all other points sampled. Hence, the method also provides a variogram (a continuous approximation of variances between any given point in the prediction area and another point) with its prediction. The variogram provides what could be used as a measure of confidence in the Kriging prediction. This comes from the fact that the fields in question contain points of interest that are geospatially autocorrelated.

4.1.2 Semi-Variogram

Kriging finds a continuous variogram by computing a discrete variogram function, a *Semi-Variogram*, from points it has actually sampled

$$\hat{\gamma}(\mathbf{h}) = \frac{1}{2N(\mathbf{h})} \sum_{i=1}^{N(\mathbf{h})} \left[Z(s_i) - Z(s_i + \mathbf{h}) \right]^2 \quad (4.2)$$

Where $N(\mathbf{h})$ is the number of pairs of data locations that are vector \mathbf{h} apart.

4.1.3 Variogram

The discrete function is then fit by a least squares to a continuous variogram that can be sampled at each point in question.

Gaussian (Normal) Kernel

Spherical Kernel

Exponential Kernel

Other Kernels

4.1.4 Choosing Kriging Weights

4.1.5 Measuring Prediction Confidence

4.1.6 Drawbacks To The Kriging Method

Although the method is optimal for data with no trends or drift, the use of the unmodified Kriging Method technique has the drawback of being computationally intensive and slow to compute in a live and timely manner. This is due to the multiple matrix inversions and least

squares fittings required to calculate the weights of the interpolation from the continuous variograms. It would be desired, in the case of autonomous UAVs that must constantly steer themselves in the best direction, to quickly calculate probabilities and variances. We will further discuss methods of efficient interpolation using the Universal Kriging Method.

4.2 Natural Neighbor Selection

4.2.1 Voronoi Tessellations

Part III

Autonomous Path Finding

We know for a geospatially autocorrelated field there is a stochastic process underlying in the data we would like to predict, and therefore could interpolate further based off of the variances of two disjoint points in the field. The variances, from samples collected in the scanning process which factor into our variogram, then become our relative confidence scores of predictions in our field in question. The values in the variogram are what will be used to terminate the interpolation when a level of least-confidence in total prediction is achieved, and what will dictate the future scan locations for a UAV or a pod of UAVs.

4.2.2 Constructing a Confidence Graph

4.2.3 Confidence Optimized Path Finding

Chapter 5

Previous Work

Some other research was once performed.

Part IV

Can it fly?

Chapter 6

Introduction

6.1 Custom Simulation

6.1.1 Flying Engine

Plot Drawing

Way-point Selection

6.2 FastPAS

6.2.1 The Algorithm

6.2.2 Simulating It

6.3 Other Uses

Chapter 7

Results

Chapter 8

Conclusion

The method has proven to be a powerful interpolation method in simulations for simulated fields. The Kriging method has proven to be a working aerial mapping technique that provides a robust model for predictions and confidence scores. The goal of this thesis will be to design the algorithm for use with a pod of autonomous UAVs. A modified technique will have to first be developed to reduce the computational complexity of the algorithm by autonomously selecting optimal neighborhoods of sub-areas to run the method on.

Once the new method has been developed, an accurate simulation demonstrating its effectiveness and potential to be used in a real pod of UAVs will then be created and demonstrated. If time and resources are available, the algorithm will be ported to a real pod of UAVs to accomplish the task of autonomous scanning using thermal imaging (via infrared sensors). Tests will be conducted to prove the effectiveness and time efficiency of the newly developed algorithm.

Bibliography

- [1] Noel A. C. Cressie. *Geostatistics*, pages 27–104. John Wiley & Sons, Inc., 2015.
- [2] Georges Matheron. Principles of geostatistics. *Economic Geology*, 58(8):1246–1266, 1963.
- [3] Harvey J. Miller. Tobler’s first law and spatial analysis. *Annals of the Association of American Geographers*, 94(2):284–289, 2004.
- [4] Donald Shepard. A two-dimensional interpolation function for irregularly-spaced data. In *Proceedings of the 1968 23rd ACM National Conference*, ACM ’68, pages 517–524, New York, NY, USA, 1968. ACM.
- [5] W. R. Tobler. A computer movie simulating urban growth in the detroit region. *Economic Geography*, 46:234–240, 1970.

Appendix A

Ancillary Material